Missouri State University

BearWorks

College of Natural and Applied Sciences

2017

K2 observations of pulsating subdwarf B stars: Analysis of EPIC 203948264 observed during Campaign 2

L Ketzer
MSU Undergraduate

Michael D. Reed
Missouri State University

A. S. Baran

P Nemeth

J H. Telting

See next page for additional authors

Follow this and additional works at: https://bearworks.missouristate.edu/articles-cnas

Recommended Citation

Ketzer, L., M. D. Reed, A. S. Baran, P. Németh, J. H. Telting, R. H. Østensen, and C. S. Jeffery. "K2 observations of pulsating subdwarf B stars: analysis of EPIC 203948264 observed during Campaign 2." Monthly Notices of the Royal Astronomical Society 467, no. 1 (2017): 461-468.

This article or document was made available through BearWorks, the institutional repository of Missouri State University. The work contained in it may be protected by copyright and require permission of the copyright holder for reuse or redistribution.
For more information, please contact BearWorks@library.missouristate.edu.

Authors

L Ketzer, Michael D. Reed, A. S. Baran, P Nemeth, J H. Telting, R H. Østensen, and C S. Jeffery

This article is available at BearWorks: https://bearworks.missouristate.edu/articles-cnas/1018

Monthly Notices
of the
ROYAL ASTRONOMICAL SOCIETY

MNRAS **467,** 461–468 (2017)
Advance Access publication 2017 January 24

doi:10.1093/mnras/stx104

K2 observations of pulsating subdwarf B stars: analysis of EPIC 203948264 observed during Campaign 2

L. Ketzer,[1⋆] M. D. Reed,[1⋆] A. S. Baran,[2] P. Németh,[3,4] J. H. Telting,[5] R. H. Østensen[1] and C. S. Jeffery[6]

[1]*Department of Physics, Astronomy and Materials Science, Missouri State University, 901 S. National, Springfield, MO 65897, USA*
[2]*Krakow Pedagogical University, ul. Podchorąży ch 2, PL-30-084 Kraków, Poland*
[3]*Astroserver.org*
[4]*Dr. Remeis-Sternwarte, Institute for Astronomy, University of Erlangen-Nürnberg, Sternwartstr. 7, D-96049 Bamberg, Germany*
[5]*Nordic Optical Telescope, Rambla José Ana Fernández Pérez 7, E-38711 Breña Baja, Spain*
[6]*Armagh Observatory, College Hill, Armagh BT61 9DG, UK*

Accepted 2017 January 12. Received 2017 January 12; in original form 2016 September 13

ABSTRACT

We apply asteroseismic tools to the newly discovered subdwarf B (sdB) pulsator EPIC 203948264, observed with *K2*, the two-gyro mission of the *Kepler* space telescope. A time series analysis of the 83-d Campaign 2 (C2) short-cadence data set has revealed a *g*-mode pulsation spectrum with 22 independent pulsation periods between 0.5 and 2.8 h. Most of the pulsations fit the asymptotic period sequences for $\ell = 1$ or 2, with average period spacings of 261.3 ± 1.1 and 151.18 ± 0.37 s, respectively. The pulsation amplitudes are below 0.77 ppt and vary over time. We include updated spectroscopic parameters, including atmospheric abundances and radial velocities, which give no indication for binarity in this star. We detect one possible low-amplitude multiplet, which corresponds to a rotation period of 46 d or longer. EPIC 203948264 appears as another slowly rotating sdB star.

Key words: stars: oscillations – subdwarfs.

1 INTRODUCTION

K2 is the extension of the very successful *Kepler* mission observing fields for ∼90 d that lie along the ecliptic plane (Howell et al. 2014). The discovery of pulsations in EPIC 203948264, observed during C2 as part of our Guest Observer proposal, is the third pulsating subdwarf B (sdBV) star observed with *K2*. Previous papers describe pulsators observed during the engineering run (Jeffery & Ramsay 2014) and C1 (Reed et al. 2016).

The unprecedented photometric data obtained by *Kepler* have proven extremely helpful for asteroseismology of subdwarf B (sdB) stars. sdB stars are located on the extreme horizontal branch with an average mass of 0.47 $M_\odot$ and temperatures ranging from 20 000 to 40 000 K (Heber 2016). They consist of a helium-burning convective core with a radiative helium-rich envelope and a very thin, hydrogen-dominated outer layer. The bulk of the hydrogen envelope is lost during the sdB star formation process. An sdB star, as a whole, represents the helium-rich inner part of most low-mass core-He burning stars, including red clump stars. The process for stripping off the envelope is not known, though binarity is the most likely cause (Han et al. 2003). Hydrogen-shell fusion cannot be sustained by their thin shells, and after leaving the horizontal branch, they proceed directly to the white dwarf cooling track without going through the asymptotic giant branch phase.

sdBV stars pulsate in both gravity (*g*) and pressure (*p*) modes. Short-period, *p*-mode pulsators, also known as V361 Hya stars, have pulsation periods between 1 and 20 min, whereas long-period, *g*-mode pulsators, or V1093 Her stars, pulsate of the order of 0.5–2 h (Østensen 2010). Hybrid pulsators have both *p* and *g* modes. *g* modes propagate from the base of the He-rich radiative zone to far out in the star, whereas *p* modes propagate only from the outer parts of this radiative zone to the surface (Charpinet et al. 2014). Rotation periods derived using *g* modes may indicate the core rotation period.

Non-radial pulsations can be classified using three quantized numbers n, ℓ and m, representing the radial overtone, the surface degree and azimuthal order, respectively (Aerts, Christensen-Dalsgaard & Kurtz 2010). Our goal is to associate modes to periodicities. From *Kepler* observations, we discovered that *g*-mode pulsations have evenly spaced periods indicative of asymptotic radial (n) overtones (Reed et al. 2011), with the $\ell = 1$ sequence having spacings of about 250 s. In addition, rotationally induced frequency multiplets have successfully been used for ℓ- and m-mode identifications (e.g. Baran et al. 2012; Baran 2012). Frequency multiplets are also useful for determining stellar rotation periods. The Ledoux rotational splitting relationship is given by $\nu_{n,\ell,m} = \nu_{n,\ell,0} + m\Omega(1 - C_{n,\ell})$ (Aerts et al. 2010), where $\nu_{n,l,m}$

⋆ E-mail: Ketzer.Laura.gmail.com (LK); mikereed@missouristate.edu (MDR)

© 2017 The Authors
Published by Oxford University Press on behalf of the Royal Astronomical Society

Downloaded from https://academic.oup.com/mnras/article-abstract/467/1/461/2949370 by guest on 29 April 2020

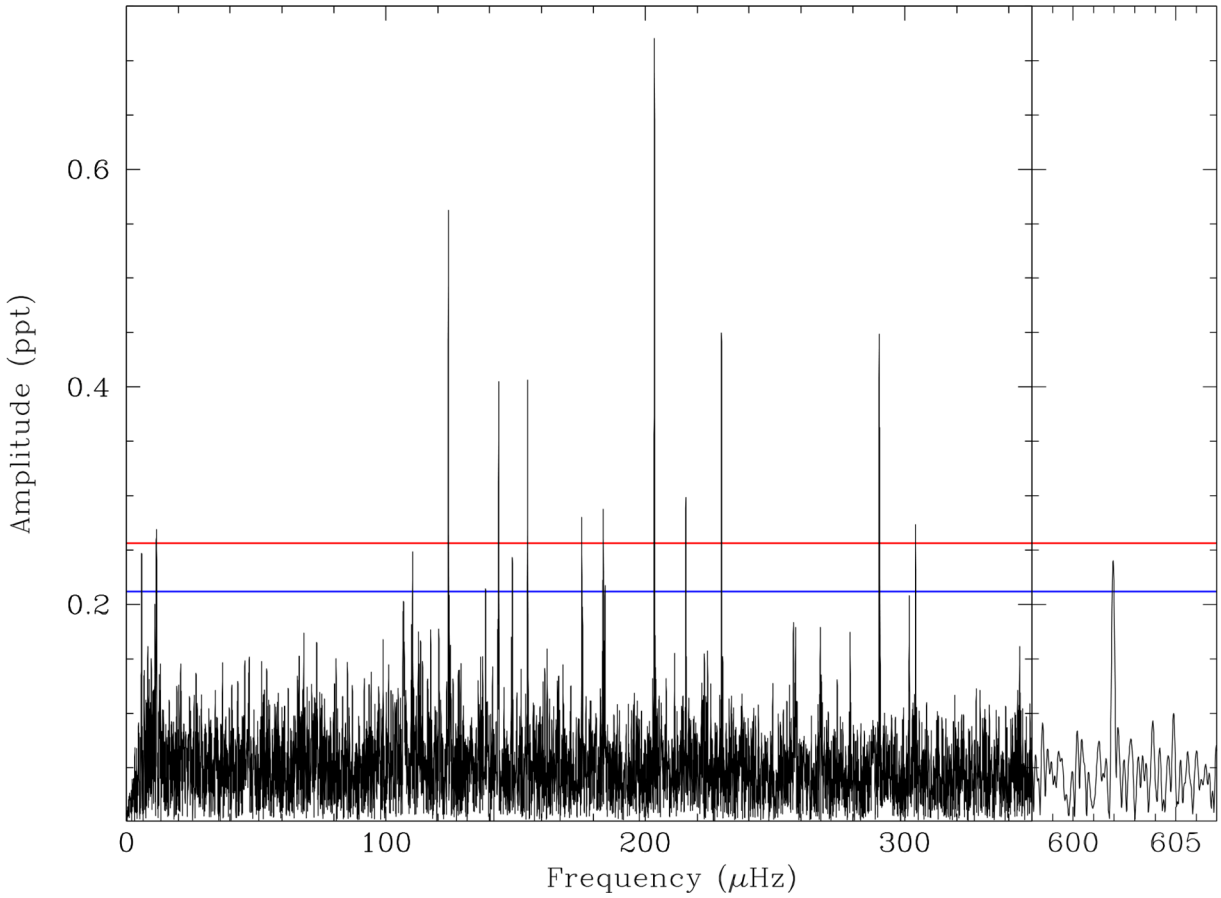

Figure 1. Fourier transform of EPIC 203948264. Horizontal blue (red) line indicates the 4.3σ (5.2σ) detection threshold.

is the observed, shifted frequency and $\nu_{n,\ell,0}$ the central frequency ($m = 0$) of the multiplet. By estimating a Ledoux constant ($C_{n,\ell} \approx 1/[\ell(\ell+1)]$ for g modes) and measuring the splittings of multiplets, we can derive a value for the rotation frequency Ω of the star. To date, all *Kepler*-observed sdBV stars have been measured to be slow rotators (Østensen et al. 2014; Reed et al. 2014; Foster et al. 2015) with periods up to 100 d including subsynchronously rotating stars in binaries (Pablo, Kawaler & Green 2011; Pablo et al. 2012; Telting et al. 2012). For a review of *Kepler* sdBV discoveries, see Reed & Foster (2014).

In this paper, we present a seismic analysis of EPIC 203948264 (J16499−2417), a g-mode pulsator with $K_p = 16.7$ discovered in *K2* data. In addition to the photometric data from *Kepler*, spectroscopy was obtained as part of our follow-up programme.

2 DATA PROCESSING AND ANALYSIS

2.1 Photometric data

The *Kepler* spacecraft obtains data in one of the two modes; the long-cadence (LC) mode produces one integration approximately every 30 min, while the short-cadence (SC) mode obtains one integration every 58.85 s. EPIC 203948264 was observed in SC mode during C2 of *K2*. The *Kepler* office is not providing processed light curves for SC data during *K2* and while several investigators are producing them in bulk (Vanderburg & Johnson 2014; Armstrong et al. 2015), we found it best to process data on a star-by-star basis. As such, we have developed a custom processing pipeline, which can be adjusted for each star. This process will be described fully in Baran et al. (2017) and we only summarize it here. We download target pixel files from the Mikulski Archive for Space Telescopes, determine coordinates for the stellar profile using Gaussians and extract aperture photometry using several sizes of round apertures that follow the star as it moves during observations. We then use custom PYTHON programs to decorrelate the pixel–brightness relationship caused by thruster firings, spline fits to remove long-term trends (>2.5 d) and select the aperture that provides the best signal-to-noise (S/N) ratio.

For comparison, we also make use of the *Kepler*-developed PYKE software packages; KEPMASK, KEPEXTRACT, KEPFLATTEN, KEPSFF and KEPCONVERT (Still & Barclay 2012). By using two independent processing methods, we could search for low-level pulsations that are consistent between both methods.

2.2 Spectroscopy

We have obtained 13 spectra between 2015 July 3–8 using the EFOSC2 spectrograph on the New Technology Telescope (NTT) at La Silla. In total, 11 spectra were obtained with grism #7 providing ∼7.4 Å resolution in the range of 3600–5100 Å and 1 arcsec slit width. Two additional spectra have been obtained with grism #19, in the range of 4400–5100 Å at a resolution of ∼1.5 Å. All spectra were obtained with two pixel binning to increase sensitivity and reduce readout time. Exposure times of the individual

Downloaded from https://academic.oup.com/mnras/article-abstract/467/1/461/2949370 by guest on 29 April 2020

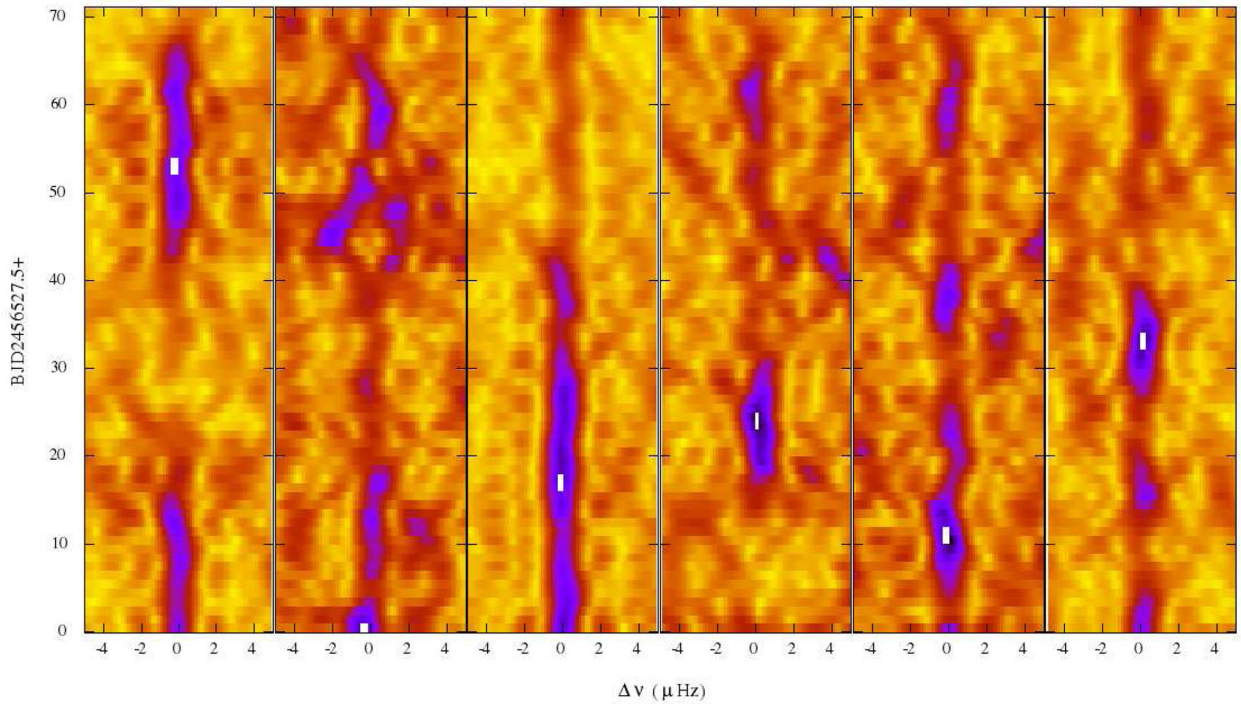

Figure 2. Series of SFTs highlighting the amplitude and frequency variability of six pulsations. From left to right: f03/04/05 multiplet (290 μHz), f08 (215.613 μHz), f09 (203.487 μHz), f11 (175.482 μHz), f12 (154.620 μHz) and f16 (124.103 μHz). Frequency is on the ordinate and time on the abscissa with colour indicating the amplitude in terms of σ. Note that each window has a different scale in which a saturated (white) pixel corresponds to 5.3σ, 3.7σ, 7.3σ, 4.5σ, 4.5σ and 6.5σ, respectively. Each individual FT spans 8 d of data with a step size of 1 d.

Table 1. List of pulsations detected in EPIC 203948264. The table provides pulsation properties, including ID, frequencies and periods with errors (Lorenzian widths) in parentheses, amplitude and corresponding S/N ratio in columns 1–5. Columns 6–10 list the mode degrees, relative radial overtone indices and the deviation from asymptotic period spacing.

ID	Freq (μHz)	Period (s)	Amp (ppt)	S/N	ℓ	$n_{\ell=1}$	$\delta P/\Delta\Pi_1$ (in per cent)	$n_{\ell=2}$	$\delta P/\Delta\Pi_2$ (in per cent)
f01	601.952 (4)	1661.262 (0.1)	0.239	4.85					
f02	304.127 (4)	3288.100 (0.5)	0.274	5.56	2			22	0.52
f03*	290.523 (4)	3442.068 (0.5)	0.276	4.01	2			23	2.56
f04[a]*	290.316 (5)	3444.523 (0.6)	0.434	6.30	2			23	4.19
f05*	290.104 (7)	3447.040 (0.8)	0.449	9.12	2			23	5.86
f06[a]	278.925 (4)	3585.193 (0.5)	0.183	3.71	2			24	2.47
f07[a]	267.444 (6)	3739.101 (0.8)	0.179	3.63	2			25	0.35
f08[a]	257.093 (6)	3889.643 (0.9)	0.183	3.72	2			26	0.89
f09	229.340 (6)	4360.338 (1.2)	0.626	9.09	1 or 2	17	10.24	29	11.15
f10	215.613 (5)	4637.939 (1.1)	0.451	6.55	1 or 2	18	4.02	31	4.87
f11	203.487 (8)	4914.319 (2.0)	0.722	14.66	1	19	1.73		
f12	183.784 (4)	5441.170 (1.1)	0.288	5.85	1	21	3.33		
f13	175.482 (6)	5698.590 (2.1)	0.279	5.66	1 or 2	22	1.83	38	1.91
f14	154.620 (6)	6467.469 (2.3)	0.569	8.27	1 or 2	25	3.96	43	7.67
f15	148.743 (5)	6723.005 (2.2)	0.343	4.98	1	26	6.18		
f16	143.517 (7)	6967.816 (3.6)	0.489	7.11	1	27	12.51		
f17	138.448 (7)	7222.928 (3.5)	0.412	5.98	2			48	8.36
f18	124.103 (5)	8057.823 (3.4)	0.769	11.18	1	31	4.58		
f19[a]	120.424 (7)	8303.993 (4.5)	0.177	3.59	1	32	0.74		
f20	110.332 (5)	9063.554 (3.8)	0.392	5.69	1	35	10.59		
f21	106.824 (10)	9361.192 (8.8)	0.344	4.99	1	36	3.30		
f22	101.104 (8)	9890.806 (7.5)	0.367	5.33	1	38	5.96		

Notes. [a]These periodicities have low S/N in our final processing, but match asymptotic spacing and thus were included in this table.
Periods labelled with * represent a potential multiplet.

Downloaded from https://academic.oup.com/mnras/article-abstract/467/1/461/2949370 by guest on 29 April 2020

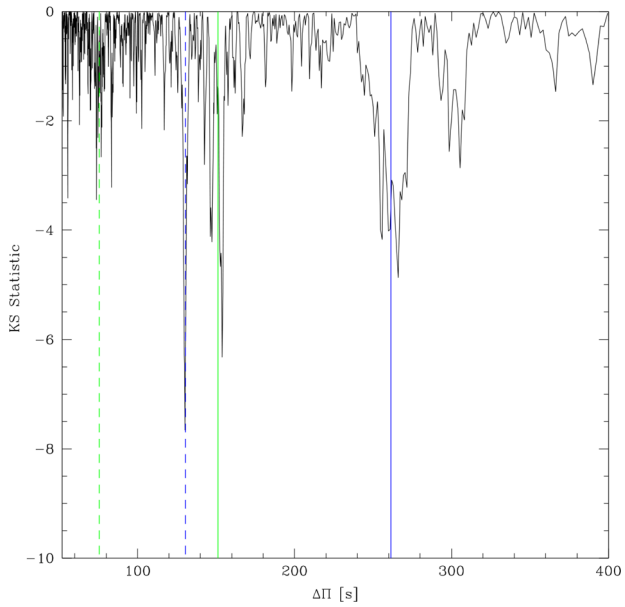

Figure 3. Output of the KS test indicating the spacing for the period sequences. The solid blue (green) line indicates the period spacing for the $\ell = 1$ (2) sequence with the dashed line being the overtone alias.

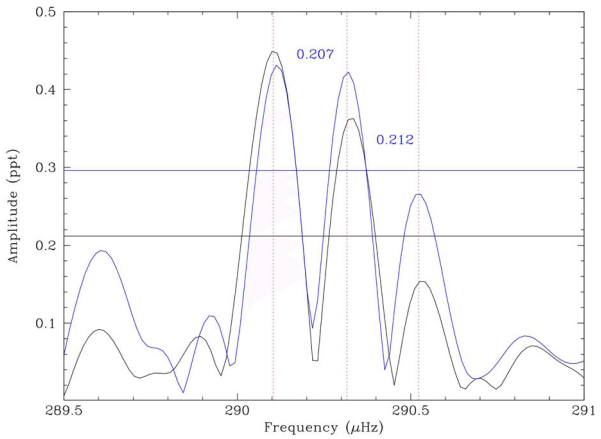

Figure 4. Possible $\ell = 2$ triplet. The black curve shows the FT obtained from our custom processing method, while the blue curve is the result of our PYKE processing. The horizontal black and blue lines indicate the detection limit for both FTs, respectively.

spectra varied between 600 and 900 s providing an S/N from 18–68. Data reduction was done using standard IRAF procedures. For wavelength calibration, helium-argon calibration frames were obtained following each science exposure.

2.3 Pulsation analysis

During C2, the spacecraft obtained data for 83 d. To ensure that the targets were properly centred in their masks, the pointing was adjusted after the first few days of the campaign. For this reason, we use only about 79 d of continuous data for our analysis. This gives us a 1/T resolution of 0.147 μHz, which corresponds to ∼56 500 independent frequencies up to the Nyquist. To make it statistically unlikely that any peaks were generated by noise requires a detection limit of 4.3σ (Bevington & Robinson 2003) or, from simulated

Table 2. Spectroscopic observations of EPIC 203948264.

Date (BJD – 2457000)	S/N	RV km s^{-1}	Error km s^{-1}
206.54138	53.1	− 5.3	8.0
206.54874	61.7	10.1	10.5
206.56254	56.8	6.0	6.6
206.56991	41.4	− 34.9	14.2
207.58364	62.4	− 21.8	8.4
207.59100	62.3	32.7	11.9
208.55276	33.0	− 4.9	11.6
208.56012	18.1	28.9	17.0
211.52451	62.1	− 10.1	7.9
211.53532	68.2	7.7	7.8

data 5.2σ (Baran, Koen & Pokrzywka 2015). The mean level of the Fourier transform (FT) was calculated to be $\sigma_{\rm FT} = 0.049$ ppt in the area of the g-mode pulsations (50–900 μHz). This sets our 4.3σ detection limit at 0.212 ppt and the 5.2σ limit at 0.256 ppt. Fig. 1 shows the frequency spectrum of the g-mode region of EPIC 203948264. The 4.3σ and 5.2σ detection limits are indicated.

From continuous *Kepler* data, we have learned that pulsations can change substantially in amplitude and show variability in frequency over time. To investigate the behaviour of pulsations in the time domain, we make use of sliding Fourier transforms (SFTs). For EPIC 203948264, we used data spanning eight days with one day steps, a portion of which is shown in Fig. 2. As in Reed et al. (2016), the SFTs show substantial amplitude variability, making traditional prewhitening ineffective. We fitted Lorentzians to the peaks to determine frequencies and amplitudes, and we use the Lorentzian widths as a measure of their net error.

We detect 17 (14) peaks in the FT above our 4.3σ (5.2σ) detection limit, and five additional peaks slightly below that. The pulsation properties are provided in Table 1. We note that frequencies/periods have not been corrected for stellar motion, which could produce shifts of the order of our uncertainties (Davies et al. 2014). The amplitudes of these five peaks lie under the justifiable detection threshold, but we include them in Table 1 because they fit the asymptotic period sequences. In total, we identify 22 pulsations ranging from 101 to 602 μHz (0.46–2.75 h). The peak (f19) at 106.824 μHz lies on top of a thruster firing artefact, but it fits the $\ell = 1$ sequence and thus was included in our analysis. The two peaks below 20 μHz are attributed to residual signals from the spacecraft that were not removed by our detrending.

We began our analysis using asymptotic period spacings to identify pulsation modes. The Kolmogorov–Smirnov (KS) test has been successfully used with sdBV stars to indicate the presence of equally spaced periods (see Reed & Foster 2014). The test produces large negative values at the most frequently observed spacing in a given data set (Kawaler 1988). Previous results on sdBV stars have confirmed that compact g-mode pulsators show evenly spaced periods, with a spacing of about 250 s for the $\ell = 1$, and 145 s for the $\ell = 2$ sequences (Reed et al. 2011). Small departures from even spacings are typically observed (e.g. Baran & Winans 2012), but are usually insufficient to disrupt sequences.

Fig. 3 shows the output of the KS test applied to EPIC 203948264's periods. The figure has troughs near 260 and 150 s and an overtone at 130 s indicating that periods are separated by these values, or multiples of them. We iteratively pick out periods with these separations, and assign relative overtones, n (assuming

Downloaded from https://academic.oup.com/mnras/article-abstract/467/1/461/2949370 by guest on 29 April 2020

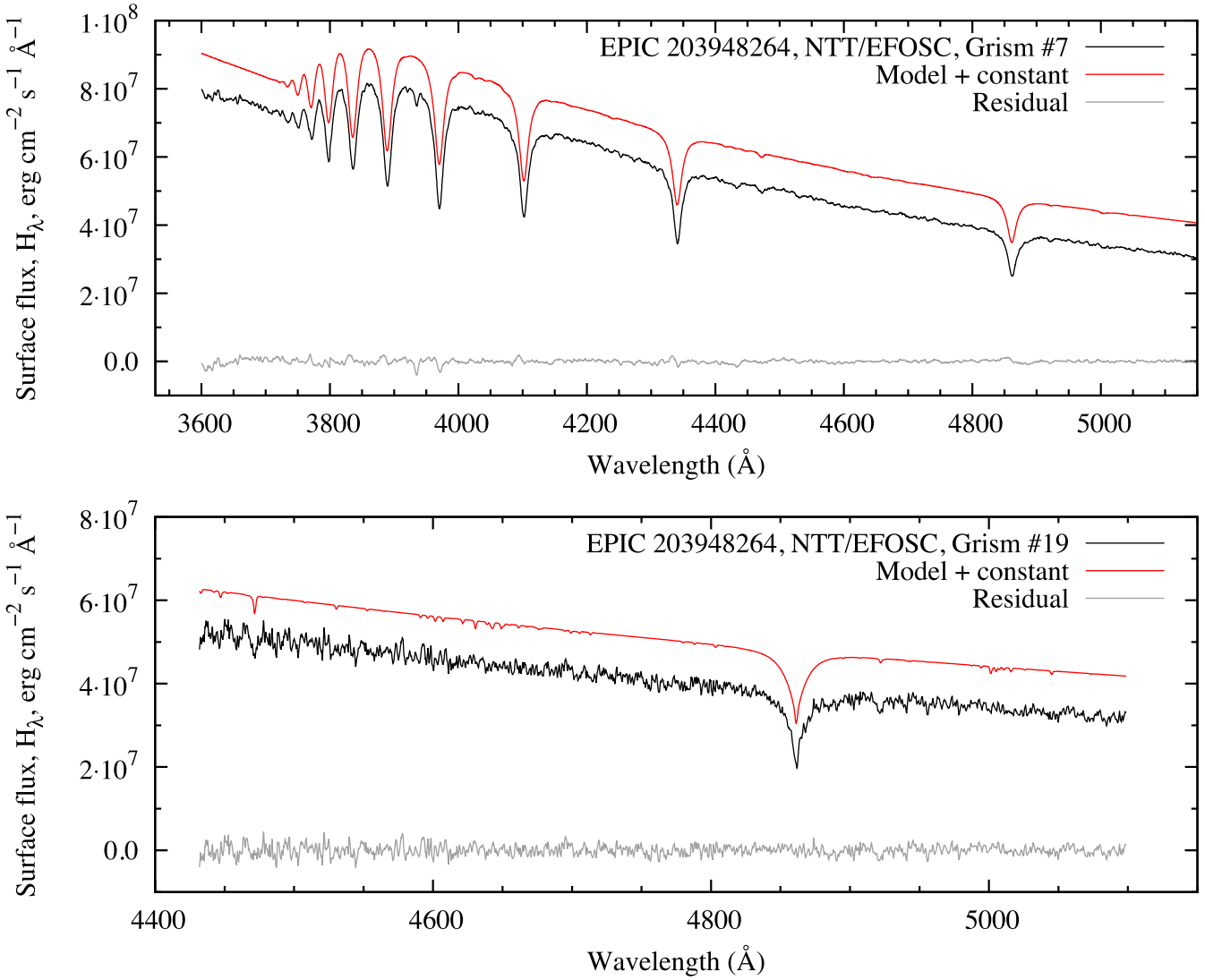

Figure 5. The combined RV-corrected NTT/EFOSC2 spectrum of EPIC 203948264 (black). The peak S/N of the combined spectrum is ∼120. The spectrum was sampled in 200 Å sections. The best-fitting model (red), computed with TLUSTY/XTGRID, is shifted vertically for clarity with residuals shown in grey. The atmospheric parameters of the model are given in Table 3.

Table 3. Parameters for the fit shown in Fig. 5, abundances relative to the solar abundances from Asplund et al. (2009) are also provided for comparison.

Parameter	Value	$+1\sigma$	-1σ	Unit	× Solar
$T_{\rm eff}$	26 760	610	700	K	
$\log g$	5.26	0.09	0.09	cm s^{-2}	
$\log n$(He)/n(H)	−2.85	0.36	0.27	dex	0.017
$\log n$(C)/n(H)	−3.84>	–	–	dex	0.54>
$\log n$(N)/n(H)	−4.27>	–	–	dex	0.79>
$\log n$(O)/n(H)	−3.66>	–	–	dex	0.45>

$m = 0$). Then we do a linear regression fit, calculate the periods for missing overtones and search for those from Table 1. In this manner, we were able to identify all of the periods as $\ell = 1$ or 2 except the shortest one, $f01$, which may not fit the asymptotic criterion $n \gg \ell$. Four of the 22 pulsation periods fit both sequences. Due to similar errors, we cannot distinguish between $\ell = 1$ and 2 for those peaks (f07, f08, f11, f12), and thus Table 1 has listings for both. The solutions of the linear regression fit find spacings of 261.3 ± 1.1 s for the $\ell = 1$ and 151.18 ± 0.37 s for the $\ell = 2$ sequences, including errors for the case of $m \neq 0$. This result is consistent with *Kepler*-observed g-mode pulsators (Reed et al. 2011) and agrees with asymptotic theory, $\prod_{\ell=2} = \prod_{\ell=1} / \sqrt{3}$ (Aerts et al. 2010). The $\ell = 1$ and 2 sequences will be discussed in terms of their echelle diagrams in Section 3.

The only possible multiplet is f03, which appears as a triplet with a splitting of 0.210 ± 0.004 μHz in Fig. 4 and is identified as $\ell = 2$ from asymptotic period spacing. This splitting is close to the formal resolution of 0.147 μHz, but it is known that phase interactions can require larger separations to resolve frequencies (Aerts et al. 2010). The amplitude of the unresolved peak is variable (Fig. 2) and we cannot distinguish between the amplitude variability creating the multiplet or beating of the multiplet creating the amplitude variability. There are only two higher amplitude periodicities in Table 1 (f09 and f16) and both are identified as $\ell = 1$. If f03 is a multiplet and f09

Downloaded from https://academic.oup.com/mnras/article-abstract/467/1/461/2949370 by guest on 29 April 2020

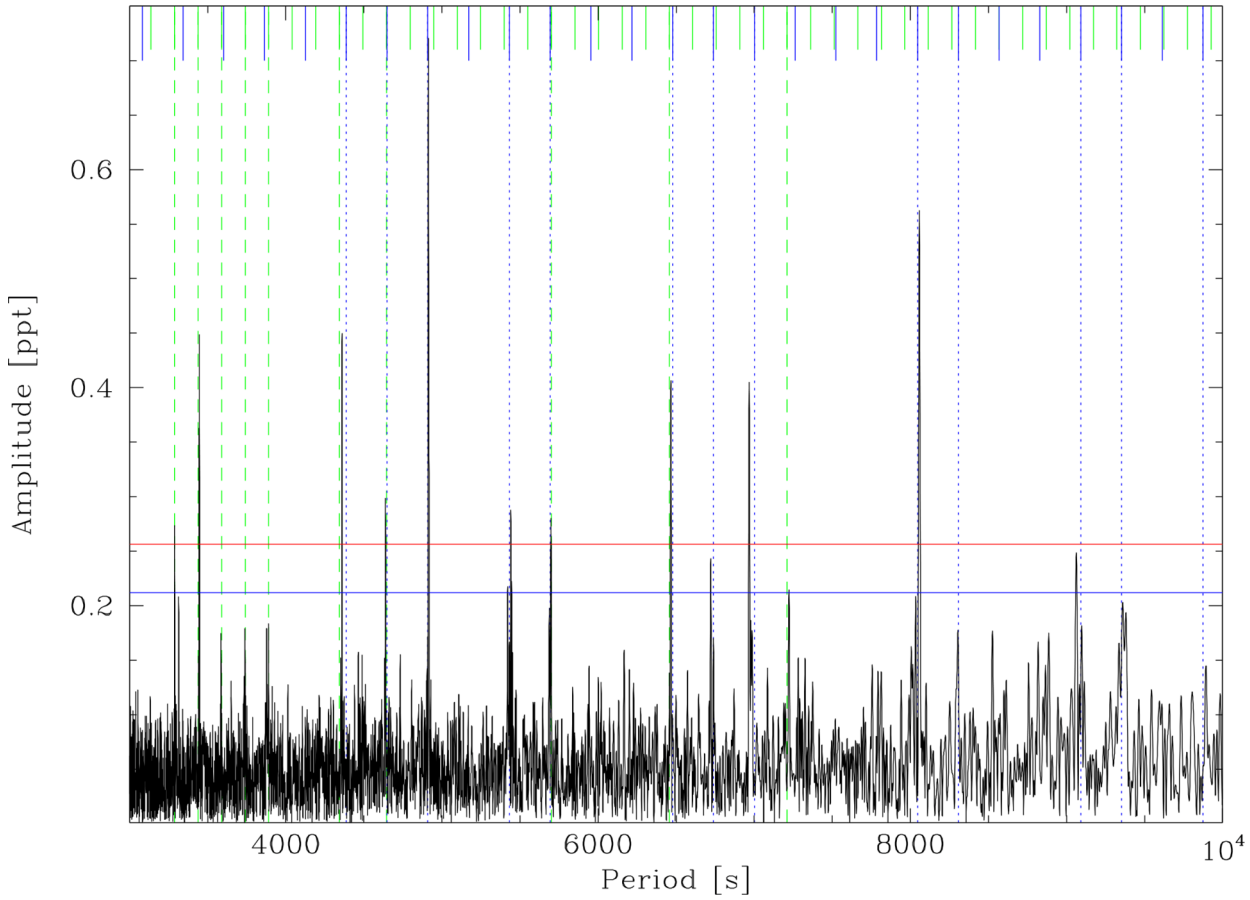

Figure 6. Period transform of EPIC 203948264 displaying the evenly spaced periods. The short blue (green) lines at the top indicate the asymptotic $\ell = 1$ (2) sequence, with the full-length dashed lines indicating the periods that match the evenly spaced sequences. Horizontal blue and red lines indicate the 4.3σ and 5.2σ detection limits, respectively.

and f16 have higher amplitudes, it could be expected that they too would be multiplets. However, given that f09 and f16 are associated with a different mode means that the other multiplet members might not be excited, the pulsation inclination is not favourable, or they are unresolved.

All seismic information is listed in Table 1.

2.4 Radial velocity measurements

We examined the 12 spectra described in Section 2.1 for signatures of binarity. The average spectrum was used as a template, with the Hβ, Hγ, Hδ, Hζ and Hη used for cross-correlation in FXCOR. The resultant radial velocities (RVs) are shown in Table 2. The RVs have two outliers, both were taken on the same night, both are part of the worst S/N spectra and these are not included in the table. If we do the cross-correlation using only the spectra with S/N > 30 then we obtain a scatter of $\sigma = 19.6\,\mathrm{km\,s^{-1}}$, which is larger than we would like, and furthermore the scatter between subsequent spectra on a single night is considerable. Still, a simple comparison with Telting et al. (2012), who found sdB binaries in the *Kepler* field, indicates that our spectra do not point at binarity for EPIC 203948264 with periods under about a day for dM companions or periods around 10 d for a WD companion. We infer that EPIC 203948264 is likely not a binary, even though our spectroscopic observations were not optimized for that purpose.

2.5 Model atmosphere analysis

To constrain the atmospheric parameters of EPIC 203948264 and estimate its metal abundance, we analysed the low-resolution NTT/EFOSC2 spectra with the TLUSTY/SYNSPEC model atmosphere and spectral synthesis codes (Hubeny & Lanz 1995; Lanz & Hubeny 2003, 2007). TLUSTY calculates fully line-blanketed, plane-parallel model atmospheres with opacity sampling and departures from local thermodynamic equilibrium (LTE) for a set of elements. We treated five elements in full non-LTE in both TLUSTY and SYNSPEC. Our models include the ions of H I, He I–II, C I–V, N I–V and O I–IV, providing 415 energy levels altogether. The spectral analysis was performed with the steepest descent iterative spectral analysis program XTGRID (Németh, Kawka & Vennes 2012). By starting out from an approximate spectral model for the sdB star, XTGRID makes successive updates of the atmospheric parameters to fit the observations and minimize the global chi-square value. The procedure does not require a model grid, new models are calculated in the direction of decreasing chi-squares. To accelerate the fitting procedure, the complexity of our models increase with the goodness of fit. The final atmosphere model is sampled in 50 depth points and converged to 0.1 per cent relative change of the structural and atmospheric parameters. Statistical errors of the final parameters are evaluated by calculating new models in one dimension until the respective confidence limit is reached. The best fit is shown in Fig. 5 and the final parameters together with error bars are listed in Table 3.

Downloaded from https://academic.oup.com/mnras/article-abstract/467/1/461/2949370 by guest on 29 April 2020

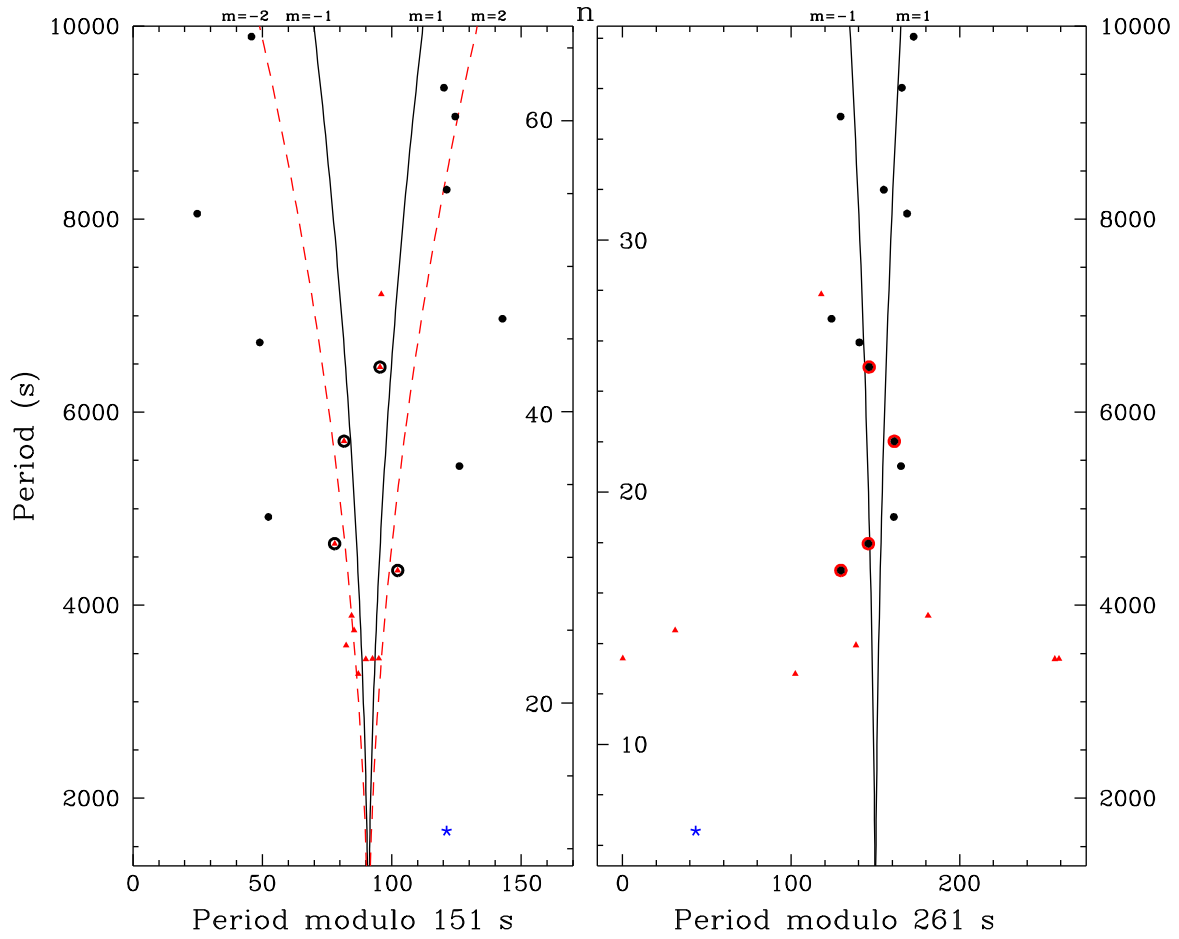

Figure 7. Échelle diagram for $\ell = 2$ modes in the left-hand panel and $\ell = 1$ modes in the right-hand panel. Periods identified as $\ell = 1$ are shown in black and these identified as $\ell = 2$ are shown in red. Periods that fit both sequences have both colours and the unidentified period is shown as a blue star. The curved lines show multiplet spacings in period, indicating periods for $m \neq 0$.

We did not find signatures of a companion in the combined spectrum, therefore we proceeded with the analysis as of a single star. Rotational velocities of sdB stars are generally low, below 10 km s^{-1} (Geier & Heber 2012). Such a low rotation velocity cannot be investigated at low resolution, therefore we did not consider stellar rotation in our models and analysis.

We found that EPIC 203948264 has a non-LTE temperature of $T_{\rm eff} = 26720 \pm 650$ K, surface gravity $\log g = 5.26 \pm 0.09$ dex and He abundance $\log(n{\rm He}/n{\rm H}) = -2.85^{+0.36}_{-0.27}$ dex, which places it well among the slow pulsating (g-mode) sdB stars. We could establish only upper limits for the carbon, nitrogen and oxygen abundances.

3 RESULTS AND DISCUSSION

We report the discovery of a new sdBV star, EPIC 203948264, from 79 d of *K2* data obtained during C2. A time series analysis of the photometric data set has revealed 22 periodicities, all but one of which we were able to associate with low-degree modes using asymptotic period spacing. Fig. 6 shows a period transform of EPIC 203948264, with the $\ell = 1$ and 2 asymptotic sequences indicated at the top and the detection limits as horizontal lines. Some of the peaks deviate from the sequence lines and this is more apparent in the échelle diagram (Fig. 7). The $\ell = 1$ sequence very clearly shows a 'hook' feature. This feature has been noticed in several sdBV stars (Baran et al. 2015), and models show some similar structures (Charpinet et al. 2014). They are attributed to a mode-trapping feature that is dependent upon evolution and envelope mass. While degeneracies in evolution and $T_{\rm eff}$–log g make discrimination complicated, as additional *K2* pulsators fill in these parameters, an ensemble analysis might be able to correlate this feature with spectroscopic quantities.

The only possible multiplet is associated with the highest amplitude $\ell = 2$ mode, which was identified using period spacings. This multiplet is only just resolved with separations of 0.210 ± 0.004 μHz. Frequency separations are typically attributed to rotation removing azimuthal degeneracy (Section 1) and so we can use this triplet to determine stellar rotation for EPIC 203948264. If $\Delta m = 1$, then the rotation period would be 45.9 ± 0.8 d and if $\Delta m = 2$ it would be 91.8 ± 1.5 d. Either of these rotation periods is similar to those measured in other apparently single sdBV stars (Reed et al. 2014). At the shorter rotation period, $\ell = 1$ multiplets would have a splitting of 0.13 μHz, and at the longer rotation period, it would be 0.063 μHz. Both splittings are below the resolution of the data that explains why no $\ell = 1$ multiplets are observed.

As in most other sdBV stars, we find variable amplitudes. Possible causes for this behaviour include beating between unresolved frequencies (as we have interpreted f03/04/05 to be), stochastic properties (as in Østensen et al. 2014) or non-linear effects such as power-switching between multiplet members (as may be occurring in KIC 106701031; Reed et al. 2014) or mode interactions (Zong, Charpinet & Vauclair 2016). Comparing the left-hand

Downloaded from https://academic.oup.com/mnras/article-abstract/467/1/461/2949370 by guest on 29 April 2020

panel of Fig. 2 with the others, f08 shows a similar time-scale of amplitude variation and f09 only has one maximum and minimum. Both of these could indicate unresolved multiplets, with f08 being $\ell = 2$ and f09 being $\ell = 1$, which would match their period spacing identifications. This does not add constraints, as those periodicities are already identified. Amplitude variations in the other periodicities do not resemble those of f03/04/05, so unresolved mode beating is not likely the cause.

We obtained follow-up spectra and determined that the non-LTE atmospheric parameters of EPIC 203948264 are consistent with slow sdBV stars: $T_{\rm eff} = 26\,720 \pm 650$ K, $\log g = 5.26 \pm 0.09$ cm s^{-2} and $\log(n{\rm He}/n{\rm H}) = -2.85^{+0.36}_{-0.27}$ dex.

Thanks to *K2* observations, EPIC 203948264 is another 'solved' sdBV star to add to the ensemble. It has determined period spacings, a 'hook' feature in the $\ell = 1$ asymptotic sequence, is apparently a single star, and has updated atmospheric parameters and abundances. EPIC 203948264 is also the only sdBV star observed during C2.

ACKNOWLEDGEMENTS

Funding for this research was provided by the National Science Foundation grant#1312869. Any opinions, findings and conclusions or recommendations expressed in this material are those of the author(s) and do not necessarily reflect the views of the National Science Foundation. ASB gratefully acknowledges a financial support from the Polish National Science Center under project No. UMO-2011/03/D/ST9/01914. This paper includes data collected by the *Kepler* mission. Funding for the *Kepler* mission is provided by the NASA Science Mission directorate. Data presented in this paper were obtained from the Mikulski Archive for Space Telescopes (MAST). STScI is operated by the Association of Universities for Research in Astronomy, Inc., under NASA contract NAS5-26555. Support for MAST for non-HST data is provided by the NASA Office of Space Science via grant NNX13AC07G and by other grants and contracts. This research has used the services of astroserver.org.

REFERENCES

Aerts C., Christensen-Dalsgaard J., Kurtz D. W., 2010, Asteroseismology. Springer-Verlag, Berlin
Armstrong D. J. et al., 2015, A&A, 579, A19
Asplund M., Grevesse N., Sauval A. J., Scott P., 2009, ARA&A, 47, 481
Baran A. S., 2012, Acta Astron., 62, 179
Baran A. S., Winans A., 2012, Acta Astron., 62, 343
Baran A. S. et al., 2012, MNRAS, 424, 2686
Baran A. S., Telting J. H., Németh P., Bachulski S., Krzesiński J., 2015, A&A, 573, A52
Baran A. S., Koen C., Pokrzywka B., 2015, MNRAS, 448, L16
Baran A. S., Reed M. D., Østensen R. H., Telting J. H., Jeffery C. S., 2017, A&A, 597, A95
Bevington P. R., Robinson D. K., 2003, Data Reduction and Error Analysis for the Physical Sciences. McGraw-Hill. New York
Charpinet S., Brassard P., Van Grootel V., Fontaine G., 2014, in van Grootel V., Green E., Fontaine G., Charpinet S., eds, ASP Conf. Ser. Vol. 481, 6th Meeting on Hot Subdwarf Stars and Related Objects. Astron. Soc. Pac., San Francisco, p. 179
Davies G. R., Handberg R., Miglio A., Campante T. L., Chaplin W. J., Elsworth Y., 2014, MNRAS, 445, L94
Foster H. M., Reed M. D., Telting J. H., Østensen R. H., Baran A. S., 2015, ApJ, 805, 94
Geier S., Heber U., 2012, A&A, 543, A149
Han Z., Podsiadlowski P., Maxted P. F. L., Marsh T. R., 2003, MNRAS, 341, 669
Heber U., 2016, PASP, 128, 082001
Howell S. B. et al., 2014, PASP, 126, 398
Hubeny I., Lanz T., 1995, ApJ, 439, 875
Jeffery C. S., Ramsay G., 2014, MNRAS, 442, L61
Kawaler S. D., 1988, ApJ, 333, 236
Lanz T., Hubeny I., 2003, ApJS, 146, 417
Lanz T., Hubeny I., 2007, ApJS, 169, 83
Németh P., Kawka A., Vennes S., 2012, MNRAS, 427, 2180
Pablo H., Kawaler S. D., Green E. M., 2011, ApJL, 740, L47
Pablo H. et al., 2012, MNRAS, 422, 1343
Reed M., Foster H., 2014, in van Grootel V., Green E., Fontaine G., Charpinet S., eds, ASP Conf. Ser. Vol. 481, 6th Meeting on Hot Subdwarf Stars and Related Objects. Astron. Soc. Pac., San Francisco, p. 45
Reed M. D. et al., 2011, MNRAS, 414, 2885
Reed M. D., Foster H., Telting J. H., Østensen R. H., Farris L. H., Oreiro R., Baran A. S., 2014, MNRAS, 440, 3809
Reed M. D. et al., 2016, MNRAS, 458, 1417
Still M., Barclay T., 2012, Astrophysics Source Code Library, record ascl:1208.004
Telting J., Østensen R., Oreiro R., Reed M., Farris L., O'Toole S., Aerts C., 2012, in Kilkenny D., Jeffery C. S., Koen C., eds, ASP Conf. Ser. Vol. 452, Fifth Meeting on Hot Subdwarf Stars and Related Objects. Astron. Soc. Pac., San Francisco, p. 147
Telting J. H. et al., 2012, A&A, 544, A1
Vanderburg A., Johnson J. A., 2014, PASP, 126, 948
Zong W., Charpinet S., Vauclair G., 2016, A&A, 594, A46
Østensen R. H., 2010, Astron. Nachr., 331, 1026
Østensen R. H., Telting J. H., Reed M. D., Baran A. S., Nemeth P., Kiaeerad F., 2014, A&A, 569, A15

This paper has been typeset from a TEX/LATEX file prepared by the author.

Downloaded from https://academic.oup.com/mnras/article-abstract/467/1/461/2949370 by guest on 29 April 2020